Journal of
Synchrotron
Radiation

ISSN 0909-0495

Received 22 May 2006
Accepted 3 December 2006

# Radiation damage to protein specimens from electron beam imaging and diffraction: a mini-review of anti-damage approaches, with special reference to synchrotron X-ray crystallography

**William H. Massover**

Department of Cell Biology and Molecular Medicine, UMDNJ – New Jersey Medical School, Newark, NJ 07101-1709, USA, and (present address) Department of Biological Sciences, Rutgers University – Newark, Newark, NJ 07102-1811, USA. E-mail: massover@andromeda.rutgers.edu

Recent research progress using X-ray cryo-crystallography with the photon beams from third-generation synchrotron sources has resulted in recognition that this intense radiation commonly damages protein samples even when they are held at 100 K. Other structural biologists examining thin protein crystals or single particle specimens encounter similar radiation damage problems during electron diffraction and imaging, but have developed some effective countermeasures. The aim of this concise review is to examine whether analogous approaches can be utilized to alleviate the X-ray radiation damage problem in synchrotron macromolecular crystallography. The critical discussion of this question is preceded by presentation of background material on modern technical procedures with electron beam instruments using 300–400 kV accelerating voltage, low-dose exposures for data recording, and protection of protein specimens by cryogenic cooling; these practical approaches to dealing with electron radiation damage currently permit best resolution levels of 6 Å (0.6 nm) for single particle specimens, and of 1.9 Å for two-dimensional membrane protein crystals. Final determination of the potential effectiveness and practical value of using such new or unconventional ideas will necessitate showing, by experimental testing, that these produce significantly improved protection of three-dimensional protein crystals during synchrotron X-ray diffraction.

**Keywords: cryo-crystallography; cryo-microscopy; electron biocrystallography; electron diffraction; electron microscopy; protein structure; radiation damage; resolution; structural biology; synchrotron X-ray crystallography; X-ray diffraction.**



## 1. Introduction

Protein structure now is determined at high resolution mainly by X-ray crystallography, neutron crystallography, nuclear magnetic resonance spectroscopy, and electron crystallography. Each approach has both strengths and weaknesses for different types of proteins and for different aspects of polypeptide structure determination. For crystallography with X-ray or electron beams, the incident radiation required to record diffraction patterns or images also causes structural changes in the protein specimens being examined; it is necessary to limit this radiation damage, in order to derive high-resolution structure for intact native polypeptides. Recent development of third-generation synchrotron X-ray sources has led to recognition that these intense photon beams are often damaging protein samples to an unacceptable extent, despite keeping specimens at a cryogenic temperature (usually 100 K) during irradiation (*e.g.* Burmeister, 2000; Ravelli & McSweeney, 2000; Weik *et al.*, 2000). Synchrotron beams also can cause damage to cryo-cooled specimens of nucleic acid crystals (*e.g.* Ennifar *et al.*, 2002). Clearly, there is a need to develop more effective approaches to counter the radiation damage accompanying synchrotron X-ray beams used for diffraction (Nave & Garman, 2005) or for scattering (Kuwamoto *et al.*, 2004).

### 1.1. Aim and organization of this mini-review

With electron beam instruments, effective countermeasures against radiation damage are in widespread use. The present text aims to deal with the important question: can any of these proven approaches to limit the effects of electron radiation damage be applied with success to synchrotron crystallography? This is a concise review, which therefore does not

attempt to be comprehensive. Since radiation damage truly is a hands-on problem, practical considerations are emphasized throughout.

An overview of the current practice of modern electron diffraction and microscopy for polypeptide structure determination will be presented first (§2 and §3), followed by a summary of protein specimen damage caused by electron irradiation (§4) and a description of the status of anti-damage countermeasures commonly used to successfully limit electron-beam-induced structural changes (§5). The key question of whether analogous approaches might be successful in improving the current radiation damage problem at third-generation synchrotron beamlines is then critically discussed (§6). Lastly, some unconventional ideas and speculations for new anti-damage approaches are presented briefly (§7); these theoretical proposals are given with the hope of stimulating examination of new directions for synchrotron experimentalists.

Excellent comprehensive reviews covering specimen damage due to electron beam irradiation are given by Henderson (1995), Glaeser (1999), and Egerton *et al.* (2004). A good summary of early studies on this important practical problem is given by Cosslett (1978). Recent results on protein structures produced by electron diffraction and imaging are reviewed by Kühlbrandt & Williams (1999), Baumeister & Steven (2000), Orlova (2000), van Heel *et al.* (2000), Chiu (2001), Frank (2002), Henderson (2004), and Chiu *et al.* (2005, 2006). The current radiation damage problem with synchrotron X-ray beams is reviewed with clarity by Carugo & Carugo (2005) and Nave & Garman (2005). Modern practical efforts to limit it are thoroughly detailed in the recent review by Garman & Owen (2006). Proceedings of the Radiation Damage Workshops [*J. Synchrotron Rad.* (2002), **9**, 327–381; (2005), **12**, 257–328] provide a good background to the increasing awareness of the importance of this problem for modern macromolecular crystallography (MX). Specialized reviews will be cited when specific topics are considered in the following text.

### 1.2. Some key differences in protein crystallography with X-rays or electrons

X-rays and electrons have a large variety of both differences and similarities. In the context of radiation damage, there are at least five very basic differences resulting in major practical consequences for their use in crystallographic studies of protein structure:

(i) size and thickness of the crystals being examined;

(ii) number of crystals needed for completion of one data-set;

(iii) conduct of cryo-protection of protein specimens;

(iv) availability of imaging and ability to obtain native structure from non-crystalline proteins; and

(v) mechanisms used for phase determination.

Despite these large practical differences, the actual crystallographic analysis has many similarities for both radiations (*e.g.* electron biocrystallographers often utilize the well developed software programs intended for use with X-ray diffraction data).

With X-ray diffraction, proteins for study must be present as well ordered three-dimensional (3-D) crystals having a typical size of some tens of micrometers. This means that diffraction intensities are produced by scattering from many thousands of unit cells [*e.g.* at least $10^{11}$ unit cells (Glaeser *et al.*, 2000)]. For transmission electron diffraction (TED), very thin crystals, only one or two unit cells thick and up to several micrometers in lateral extent, are necessary; thicker crystals cannot be used because multiple scattering of the transmitted electrons must be avoided. The form of these thin specimens means that electron diffraction intensities come from scattering by many fewer unit cells (*e.g.* only some hundreds or thousands), as compared with the genesis of X-ray diffraction intensities. With modern cryo-MX, a complete data-set often can be collected using only one good crystal. With TED of thin protein crystals, at least many dozens or hundreds of different crystals must be used in order to obtain a complete data-set containing intensities from many different angles of incidence; this means that electron biocrystallography often takes many months to complete the data collection for each structural study.

Protein specimens for use with either radiation now usually are cooled with a liquid or gaseous cryogen, providing cryo-protection to reduce the effects of radiation damage. Thick crystals for X-ray diffraction must first be treated with a cryo-protectant before cooling, in order to avoid structural damage from the crystallization of water (in the mother liquor permeating the crystal volume). Monolayer or bilayer crystals used for electron diffraction can usually be prepared within a very thin layer of aqueous solution, thereby permitting successful vitrification to form amorphous ice or frozen buffer; thus, no cryo-protectant agents are needed or used with such specimens. The cooling rate is slower and the cryogen consumption is higher for thick protein crystals than for very thin crystals.

Electron beams are readily used for imaging, as well as for diffraction, by virtue of the electromagnetic lenses in electron microscopes. The availability of imaging with transmission electron microscopy (TEM) is a very important research capability for two quite different reasons. First, it permits high-resolution structural studies to use individual uncrystallized protein molecules and assemblies as specimens; with TEM, crystallization is not required. The images represent randomly oriented two-dimensional (2-D) projections, which can be computer processed to determine the spatial orientations of each in the many thousands of imaged particles recorded, thereby permitting their merging into one reconstructed 3-D structure. The major practical limitations of imaging with TEM concern obtaining an adequate number of imaged particles that are undamaged during specimen preparation and irradiation. Use of soft or hard X-rays for imaging is currently the subject of developmental experiments, but is not routinely available at present; new paradigms for using X-rays from synchrotrons or free-electron lasers (*e.g.* Miao *et al.*, 2000) with holography (*e.g.* Novikov *et al.*, 1998; Adams *et al.*,

2000; Eisebitt *et al.*, 2004) or diffractive imaging (*e.g.* Miao *et al.*, 2001; Huldt *et al.*, 2003; Chapman *et al.*, 2006) might be able to provide X-ray images of protein specimens that are much less compromised by radiation damage.

A second major feature of the ability to obtain high-resolution images with electron beam instruments is that phases can be determined directly from images of samples of the crystals being diffracted (*i.e.* TEM images contain both phase and amplitude information). For X-ray diffraction studies, phase determination usually comes from measurements of anomalous dispersion caused by the presence of strongly scattering atoms associated with or within the polypeptides of each unit cell. Most commonly, this requires preparation of heavy-atom derivatives, or incorporation of modified amino acids (*e.g.* selenomethionine) into recombinant polypeptides; although widely used, these approaches to phasing for X-ray diffraction are not always available or successful. The presence of these dual capabilities with TEM imaging guarantees that this mode of structure determination will continue to be utilized, despite the fact that TED approaches achieve better resolution levels.

The separate pathways taken for polypeptide structure determination with the two radiations have recently been coming together, as exemplified by the increasing use of merging high-resolution X-ray structures for component polypeptides into medium-resolution structures for large macromolecular assemblies (see §3). Wider use of this combined approach to determining large-scale protein structures at high resolution is forming a very powerful direction for modern structural biology; the research value of using complementary approaches is particularly well illustrated by recent advances in the structure and function of ribosomes (see reviews by Liljas, 2006; Mitra & Frank, 2006).

### 1.3. Why should synchrotron crystallographers have interest in technical experiences with electron biocrystallography?

Radiation damage to protein specimens is the most fundamental practical problem and limitation for crystallographers using either X-rays or electrons. Available information about the actual physico-chemical mechanisms causing radiation-induced structural damage to polypeptides (see §4) indicates a common final pathway for these changes coming from both X-rays and electrons (Henderson, 1990; Glaeser *et al.*, 2000). As stated by Glaeser *et al.* (2000), "damage caused by X-ray exposures is really damage caused by electrons". Hence, effective approaches developed for either radiation are likely to produce beneficial effects for the other; this is exemplified by the widespread use of cryo-cooling with both radiations. Anti-damage measures developed and proven successful by workers using TEM and TED may be transferable; development of effective improvements for the unsolved radiation damage problems with synchrotron X-ray diffraction will be facilitated by having an open mind and a willingness to consider new ideas and unconventional approaches.

## 2. Specimen preparation for electron crystallography

Recombinant or natural protein samples are commonly prepared for examination by TED or TEM using either of two different methods (see reviews by Yaeger *et al.*, 1999; Saibil, 2000; Ruprecht & Nield, 2001).

(i) *Frozen-hydrated specimens.* Single particles (*e.g.* polypeptide molecules, oligomers, supramolecular assemblies, viruses, subcellular structures) or thin 2-D crystals (*i.e.* highly ordered monolayers or bilayers) suspended or dissolved in a dilute buffer or water are used as specimens. A droplet is applied onto one side of a fenestrated (*i.e.* where random orientation is desired) or continuous (*i.e.* where directed orientation is desired) thin carbon film covering a grid. Following blotting with filter paper, the thin aqueous layer left overlying the support film and bridging any holes is plunged into liquid ethane, where it freezes so rapidly that water is vitrified (see reviews by Adrian *et al.*, 1984; Dubochet *et al.*, 1988). The frozen specimen grid with protein samples inside a thin layer of vitreous ice is transferred into liquid nitrogen or helium and is then inserted into a submerged special shielded holder kept at the temperature of liquid nitrogen or liquid helium. This is finally transferred into the high vacuum inside a transmission electron microscope, where the low temperature of the specimen is maintained by direct thermal coupling of the specimen holder through metal connections to a reservoir of liquid cryogen. With frozen-hydrated samples, the very low temperature of liquified nitrogen or helium is used both to prevent sublimation of ice into the surrounding high vacuum and to provide temperature-based protection during subsequent imaging or diffraction.

(ii) *Supported-dried specimens.* A droplet containing single protein particles or 2-D crystals is deposited onto a continuous or fenestrated thin carbon support film. Following blotting to remove most of the applied liquid, a drop of a structure-supporting sugar (*e.g.* glucose, tannin, trehalose) in aqueous solution is added to the wet preparation (*e.g.* Unwin & Henderson, 1975; Hirai *et al.*, 1999). After removal of most of this liquid by blotting, the entire preparation is then dried in air; the thin layer of dilute solution of structure-preserving sugar dries into a glassy state. Sugars form many hydrogen bonds with polypeptides in the wet sample during dehydration, and by this and other mechanisms prevent polypeptide denaturation upon drying (Allison *et al.*, 1999; Crowe, 2002; Kaushik & Bhat, 2003). Experimental studies have shown that different labile enzymes dried within a sugar matrix retain substantial or even full catalytic activity when rehydrated (Lippert & Galinski, 1992), and retain their catalytic specificity (Uritani *et al.*, 1995); dehydration-induced conformational changes are inhibited by the presence of structure-preserving sugars, thus preventing denaturation and inactivation (Prestrelski *et al.*, 1993). Most commonly, the fully dried preparation is then immersed into liquid cryogen, moved into a transfer device, inserted into the microscope, and maintained at cryogenic temperature during subsequent imaging or diffraction, thereby providing cryo-protection to the dry proteins.

Both the frozen-hydrated (*e.g.* Ren *et al.*, 2000; Yonekura *et al.*, 2005) and the sugar-supported dry (*e.g.* Wang & Kühlbrandt, 1991; Löwe *et al.*, 2001) types of specimen preparations can yield high-resolution polypeptide structure. Recently, a hybrid approach has been developed, whereby trehalose-immersed, but still wet, specimens are vitrified (Gyobu *et al.*, 2004); these frozen-hydrated specimens have given very good results for several membrane proteins (Kimura *et al.*, 1997; Gonen *et al.*, 2005).

## 3. Current status of protein structure determination by electron crystallography

Natural or recombinant membrane proteins sometimes can be manipulated to form very thin highly ordered 2-D crystals (*e.g.* Jap *et al.*, 1992; Kühlbrandt, 1992), thereby enabling the most successful and important application of electron biocrystallography to structural biology (see reviews by Fujiyoshi, 1998; Henderson, 2004). This capability is fortunate, since X-ray crystallography traditionally has major problems in dealing with this very largest class of polypeptides (Fleishman *et al.*, 2006).

At present, the best resolution level reported by electron crystallography is 1.9 Å, recently shown for a 3-D structure determination of 2-D crystals of the membrane protein, aquaporin-0 (Gonen *et al.*, 2005), with the use of liquid helium cryo-protection. An example of one of their low-dose electron diffraction patterns is reproduced in Fig. 1; the Bragg spots extend to angles even higher than the reported nominal resolution level. Diffraction patterns from frozen-hydrated specimens tilted to over 70° in this study are almost as extensive as the high-quality untilted example shown here (Gonen *et al.*, 2005); since radiation damage prevents data collection from any one crystal for all the tilt angles required in crystallographic analysis, the complete 3-D data-set for this recent study required diffraction measurements to be made on several hundred crystals. This high-resolution structure analysis was also able to determine the position of seven annular lipids and two bulk lipids around the transmembrane polypeptide (Gonen *et al.*, 2005). A variety of other membrane proteins (Fujiyoshi, 1998, 2006; Henderson, 2004) and crystalline non-membrane proteins (*e.g.* Löwe *et al.*, 2001) have now been determined to a resolution level of 3–4 Å, using specimen protection with either liquid nitrogen or helium.

For imaging studies with single particles, very large numbers of individual samples (*e.g.* at least several tens of thousands) must each have their 3-D orientation determined before a full high-resolution structure can be derived. TEM imaging of these unstained samples relies on the use of electron phase contrast; the strong defocus needed to increase phase contrast in turn requires computer-based correction of the contrast transfer function during image processing and analysis. At present, the best resolution level reported for non-viral single particle specimens is a recent structure determination of the GroEL chaperonin complex at 6.0 Å (Ludtke *et al.*, 2004). Fig. 2 shows the GroEL polypeptide structure reconstructed from imaging of single particles within a layer of vitreous ice. This structure necessitated merging image data for almost 40000 individual particles recorded on 42 different micrographs. It is very similar to the corresponding structure independently derived using X-ray diffraction data from 3-D crystals (Braig *et al.*, 1995), after they are truncated from 2.8 Å to the same 6.0 Å resolution level; detailed comparisons show that most $\alpha$-helices can be positively identified in the cryo-

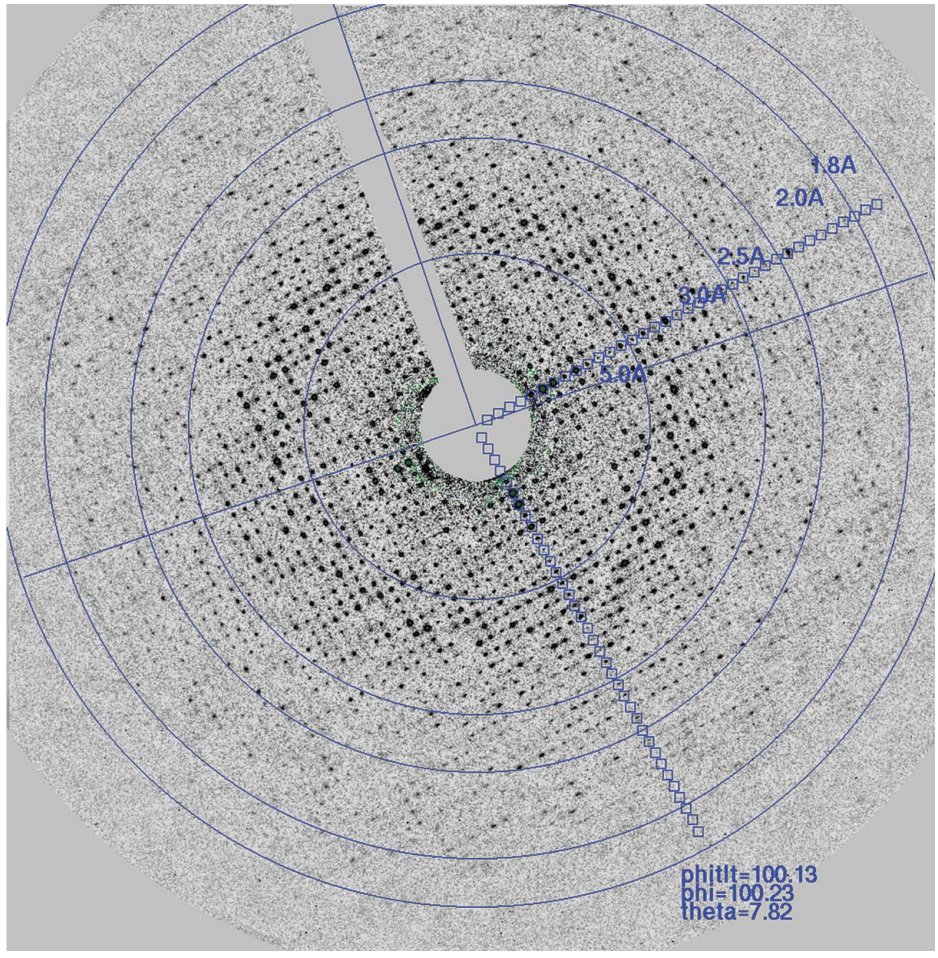


**Figure 1**
A typical electron diffraction pattern recorded from an untilted AQP0 2-D crystal prepared by the carbon sandwich technique (Gyobu *et al.*, 2004), showing diffraction spots to a resolution beyond 2 Å. [Reproduced with permission from Fig. 1(*b*) of Gonen *et al.* (2005), *Nature (London)*, **438**, 633–638.] The specimen is cooled by liquid helium.

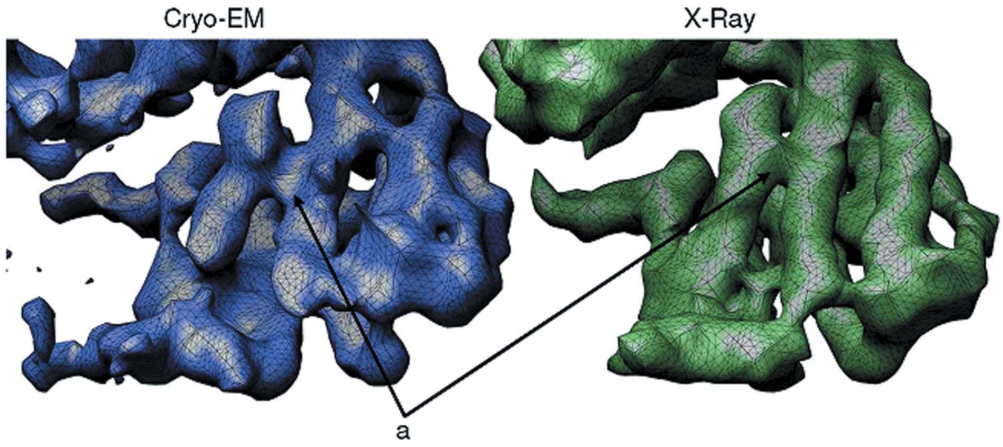


**Figure 2**
Isosurface rendering of the equatorial domain of the single particle reconstruction (left, blue) and the docked crystal structure filtered in the same way as the single particle reconstruction (right, green). The arrows indicate one point where the helices are apparently bridged in both structures. At higher isosurface thresholds this bridge can be eliminated in both structures. [Reproduced with permission from Fig. 5 of Ludtke *et al.* (2004), *Structure*, **12**, 1129–1136.]

**Table 1**
Major mechanisms and consequences of electron beam radiation damage to polypeptide structure.

| Major mechanisms of radiation damage | Consequences for the protein specimen |
|---|---|
| Heating | Melting; mobility; change in configuration |
| Ejection of mass | Mass loss; mass redistribution |
| Breakage of covalent bonds | Changes in atomic positions; mobility |
| Charge alteration and ionization | Changes in native charge distribution |
| Generation of free-radicals | Secondary effects modifying specimens |

TEM map (Ludtke *et al.*, 2004), as can 23 C-terminal residues that were not included in the X-ray crystal structure (Braig *et al.*, 1995). Some small differences between the two reconstructions also can be discerned in Fig. 2, and are probably due mainly to the different types of specimens being examined; individual polypeptides in X-ray diffraction studies all have an identical orientation and are rigidly locked into a large 3-D lattice, but the uncrystallized protein molecules in electron imaging studies are independently oriented and have a much larger degree of conformational flexibility.

The protein shell of non-crystallized viruses can now be determined to around 6 Å with phase-contrast imaging of frozen-hydrated specimens (see reviews by Steven *et al.*, 1997; van Heel *et al.*, 2000; Chiu & Rixon, 2002; Chiu *et al.*, 2005). The icosahedral or other internal symmetry present within many virus shells decreases the number of imaged single virions needed to reconstruct the capsid polypeptide structure. Certain other non-viral protein specimens can be ordered into helical arrays, either naturally (*e.g.* bacterial flagellin; Yonekura *et al.*, 2005) or with laboratory manipulation (*e.g.* nicotinic acetylcholine receptor; Unwin, 2005); the helical symmetry advantageously permits simultaneous recording of multiple different rotational projections within each image (DeRosier & Moore, 1970; Owen *et al.*, 1996).

For very large protein complexes containing many different polypeptides (*e.g.* ribosomes), increasing use is being made of a hybrid approach, where atomic level structures for the component polypeptides coming from X-ray diffraction are docked (merged) within a moderate resolution structure for the entire large complex derived from TEM imaging (*e.g.* Glykos *et al.*, 1998; Steinmetz *et al.*, 1998; Belnap *et al.*, 1999; Harms *et al.*, 1999; Wriggers *et al.*, 1999; Rossman *et al.*, 2001, 2005; Tang & Johnson, 2002; Wu *et al.*, 2003; Fabiola & Chapman, 2005; Mitra & Frank, 2006). The resulting hybrid reconstructions usually have an overall resolution level that is intermediate between those of the separate components.

## 4. Radiation damage to protein specimens during electron beam imaging and diffraction

The ultimate goal of structural biology is to determine *native* polypeptide structure and thereby to provide a structural basis for understanding molecular function and dynamics. Any damage to polypeptide structure from specimen preparation or irradiation necessarily compromises achieving this goal. Electron microscopists have been aware that transmitting electrons through proteins damages them, ever since the earliest days when heating and ashing of biological samples were observed frequently. Electron-beam-induced specimen damage, just as X-ray radiation damage, can be subdivided into two categories: primary and secondary. Primary damage results from interactions between the incident electrons and atoms in polypeptides or in their surrounding matrix. Secondary damage results from interactions between protein specimens and the free-radicals produced during the primary damage events.

Today it is clear that the energy deposited into protein specimens comes from inelastic electron scattering events, both for X-ray and electron irradiation (Henderson, 1995, 2004; Glaeser *et al.*, 2000). The general consequences of radiation damage to polypeptides from transmitted electrons are outlined in Table 1. Any breakage of covalent bonds, mass loss, or alteration of natural charge distribution often have large and undesired effects on polypeptide structure determination; the result of either primary or secondary damage necessarily is that the reconstructed high-resolution structure

shows a non-native state. Fortunately, much of this beam-induced damage can be limited to a given level of resolution by using the means described in §5. The recent improvement in TEM resolution with membrane protein crystals to 1.9 Å (Gonen *et al.*, 2005) undoubtedly signifies that renewed attention to the detailed effects of electron radiation damage is necessary to further advance the routine resolution level beyond its present range of 3–6 Å.

## 5. Common approaches taken to limit electron beam damage to protein specimens

Following long research experience up to the present, three main approaches in TEM and TED have been developed to counter and limit specimen damage during the irradiation needed for specimen observation and data recording (Table 2). Some countermeasures are effective in reducing both primary and secondary damage. The practical goals for data recording are to use the necessary irradiation very efficiently and to keep the radiation-induced changes to some minimum that then permits a given level of high-resolution structure to be derived.

### 5.1. Changes in instrumentation

New electron microscopes intended for structural biology research are now equipped with higher accelerating tension (300–400 kV), a field emission electron gun, and a cryo-transfer device and cryo-specimen holder using liquid helium (or liquid nitrogen). In some cases, yet other special instrumentation features might be added to this basic list. Electrons at 300–400 kV have a faster velocity and a shorter wavelength than those at the traditional accelerating voltage of 50–100 kV. These electrons interact with fewer atoms in polypeptides of the specimen, thereby decreasing the radiation damage. However, this decreased scattering is accompanied by a reduced level of signal containing the structural information, and by a decrease in detector performance. The signal-to-noise ratio (SNR) is maintained and the final balance remains positive, due to a decreased number of double-scattering events, lower curvature of the Ewald sphere, and reduced influence of specimen charging, as compared with the use of lower accelerating voltages (Henderson, 1995). Although megavolt electron microscopes are also available, these are not used to study protein structure due to their production of considerable knock-on damage (*e.g.* Henderson, 1995), whereby transmitted electrons directly eject atoms from the sample, resulting in mass loss. Carbon and other light atoms in proteins are not removed very significantly until the accelerating tension reaches 200 kV (Egerton *et al.*, 2004); use of very limited electron doses helps limit the influence of mass loss when working at 300–400 kV.

All modern instruments have facilities for high-resolution digital data recording of diffraction patterns and images [*i.e.* a charge-coupled device (CCD) camera, or an imaging plate]. Both are particularly suitable for recording low-dose electron diffraction patterns, due to their large dynamic range. CCD cameras have the advantages of very high sensitivity to electrons, and a linear response (see review by Faruqi & Subramaniam, 2000). These detector capabilities are particularly advantageous for data collection when electron beams must be kept at very low intensities (*i.e.* low-dose recordings), thereby facilitating a reduction of radiation damage (see §5.2). Where photographic film is selected (*i.e.* for recording of imaging data), a high-resolution scanning densitometer is used to convert these analog images into a digital format. The most important practical advantage of film over present CCD chips is that it has a much larger recording area, thereby registering many more pixels. With further technical advances, the properties of CCD cameras may soon equal the good capabilities of photographic film, so they then will also be used routinely for acquisition of low-dose imaging data.

**Table 2**
Main effects of anti-damage approaches upon protein specimens subjected to electron diffraction and imaging.

| | | Main action on | |
|---|---|---|---|
| Anti-damage approach | Chief effect on specimens | 1° damage | 2° damage |
| Higher accelerating tension | Fewer interactions with specimen atoms | Reduced | Reduced |
| Low-dose exposure | Less radiation dose | Reduced | Reduced |
| Cryo-protection | Specimen remains cold; fragments and free-radicals immobilized | | Reduced |
| Protective matrix | Quenches free radicals | | Reduced |

Almost all adjustments for actual operation of electron microscopes and data collection are now controlled through computer software available from instrument manufacturers and from several other commercial vendors. Several laboratories recently have developed software to provide full automation of specimen area evaluation and selection, beam and focus adjustment, and data recording (*e.g.* Suloway *et al.*, 2005; Lei & Frank, 2005); comparable software is now becoming commercially available. Such automation will be particularly significant for unattended recording of all the many images needed to characterize the structure of numerous recombinant polypeptides. Stagg *et al.* (2006) have just reported use of this automation to record cryo-TEM images containing 284742 single particles of the GroEL protein complex; these very extensive data were able to be collected within a single session of 25 h. Spot-scan exposures (Downing & Glaeser, 1986; Bullough & Henderson, 1987; Downing, 1991) are enabled by software control of electron beam size and positioning; this protocol is readily applicable where specimen grids have a regular pattern of holes, thereby reducing specimen heating and charging by subjecting only these limited small areas to the irradiation. Software must be considered to be an important additional component in the efforts of instrumentation to limit specimen damage.

### 5.2. Low-dose exposures for imaging and diffraction

Since the same electron beam that is elastically scattered by polypeptide atoms to produce the recorded structural data is also inelastically scattered and thereby imparts energy into

the specimen, it is impossible to totally eliminate radiation damage. However, the amount of primary and secondary radiation damage can be reduced by limiting the number of incident electrons to the minimum needed to record the structural information with statistical validity; this concept of 'low-dose exposure' was first fully developed by Unwin and Henderson in their classic report on studies of purple membranes and catalase crystals (Unwin & Henderson, 1975). Low-dose recording of both imaging and diffraction data is now performed with computerized control by standard commercial software packages, and is adopted universally for investigations in structural biology.

For practical use with electron beams, low-dose exposures of both images and diffraction patterns have four essential features. First, there should be either no or only some minuscule pre-exposure to the electron beam (*i.e.* during selection and centering of specimens). Second, adjustment of focus is performed off-axis (by means of beam deflectors which direct the narrow spot of electrons through some neighboring area several micrometers distant from the on-axis crystal or area of interest). Third, recording of the on-axis specimen includes the very first transmitted electrons, since these will come from the undamaged specimen. Fourth, the total exposure to the electron beam is limited to that required to produce the minimally adequate SNR. For this to be accomplished routinely, computer-controlled beam blanking completely prevents any specimen irradiation except when the exposures are activated.

Although low-dose recording necessarily produces weak and noisy images of single particles, the SNR can be increased subsequently by summing many separate imaged objects into a composite after intensity normalization and sorting during image processing. For low-dose images of thin crystals, the SNR is increased by Fourier processing. Failure to obtain the required minimal SNR produces images where boundaries, internal substructure, and orientations of single particles are not sufficiently defined above the noise level; that prevents rigorous determination of their position and orientation, as needed to reconstruct 3-D structure at high resolution. To combat the weak signal level in low-dose images, the fourth requirement sometimes is modified, by recording the first transmitted electrons along with enough additional electrons to give a moderate level of contrast; such data thereby include information from both undamaged and damaged structures.

How much can the necessary electron beam exposure be reduced? To answer this question, Glaeser and colleagues (*e.g.* Hayward & Glaeser, 1979; Glaeser, 1999) have used the Rose criterion (Rose, 1948) which states that the standard deviation of the signal must be at least five times the noise level to be statistically valid. At this limiting SNR, low-dose images often have no visible content at all when examined with the naked eye; the recorded structural information is recovered through the use of Fourier analysis for diffraction from crystals, and of computer-driven classification analysis and merging for single particle data. Low-dose diffraction patterns must record the very highest angle Bragg spots with the required minimal SNR, meaning that all the many reflections for larger spacings are simultaneously being recorded with a higher SNR.

What is the maximum electron beam exposure that can be tolerated before structural damage becomes unacceptable? The answer to this question depends generically upon the resolution being sought (Henderson, 1995; Glaeser, 1999). For studies at high resolution, Henderson has used available quantitative measurements to calculate (see derivation by Henderson, 1990) that the electron beam radiation dose causing the destruction of half the diffracted intensity is around 5 e $Å^{-2}$ (for 100 kV electrons interacting with protein specimens maintained near the temperature of liquid nitrogen). This corresponds to a dose of around $5 \times 10^7$ Grays [Gy: units of energy deposited per unit of mass (*i.e.* Joules per kilogram)]. This limit of 5 e $Å^{-2}$ predicts that structural damage to biological specimens should be apparent at any higher dose; in fact, somewhat larger doses (*e.g.* 10–25 e $Å^{-2}$) often can be tolerated for TED and TEM with the addition of higher accelerating tension and cryo-protection. Henderson (1990) also calculated a predicted dose limit to half diffraction intensity of $2 \times 10^7$ Gy for synchrotron X-ray beams; an experimental evaluation of this limit based on synchrotron X-ray measurements with protein crystals by Owen *et al.* (2006) has concluded that the recommended safe dose is about 50% greater ($3 \times 10^7$ Gy) than that earlier calculation, and corresponds to 0.7 of the initial diffraction intensity remaining.

### 5.3. Low-temperature-based protection of specimens

Electron cryo-microscopy (see reviews by Grimes *et al.*, 1999; Kühlbrandt & Williams, 1999; Saibil, 2000; Subramaniam & Milne, 2004; Chiu *et al.*, 2005) uses instruments that are specially constructed to maintain specimens at cryogenic temperature during their examination and data recording. Cryo-protection in TEM denotes the low-temperature-based preservation of protein specimens against radiation damage; this usage corresponds to the term 'cryo-cooling' in MX (*i.e.* no chemical additives are utilized). Cryo-protection is separate from a frozen-hydrated status (*i.e.* when cooled, even dry specimens receive the temperature-based protection against radiation damage). This low-temperature-based protection (see reviews by Henderson, 1990; Fujiyoshi, 1998) is commonly believed to act against any beam-induced heating, reduce mobility of beam-generated free-radicals (Henderson, 1990), and hinder redistribution of atoms or molecular fragments liberated from the specimen by the irradiation. For both electron and X-ray beams, cryo-protection increases the radiation dose that can be utilized before significant structural changes occur.

Electron cryo-microscopes using liquid helium instead of liquid nitrogen (Fujiyoshi *et al.*, 1991) have now become commercially available. There is a long history of ongoing controversy about the anti-damage capabilities of liquid helium *versus* liquid nitrogen with TED/TEM (*e.g.* International Study Group, 1986). Even in 2006, liquid helium was reported to be less beneficial than liquid nitrogen for certain uses in electron microscope tomography (Comolli & Downing,

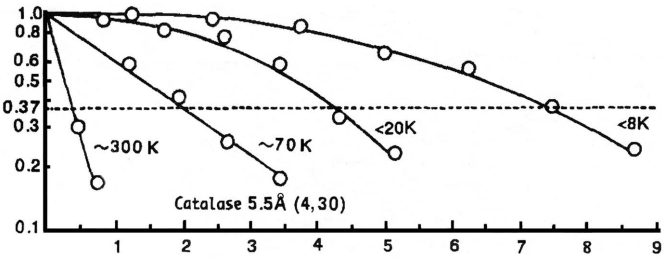


**Figure 3**
Irradiation damage of catalase crystals. The fading of the intensities of the diffraction spots (4, 30) is plotted as a function of the accumulated electron dose. This plot demonstrates that a further reduction of the specimen temperature from liquid-nitrogen to liquid-helium temperature results in an improvement of the cryo-protection factor by two or more. [Reproduced with permission from Fig. 4 of Fujiyoshi (1998), *Adv. Biophys.* **35**, 25–80.] Vertical axis: relative intensity of diffraction spot; 1.0 on scale = 100%. Horizontal axis: total accumulated radiation dose in e $Å^{-2}$; the dotted line at 0.37 is placed at 1/e, which often is used for determining the critical dose.

2005; Iancu *et al.*, 2006). Nevertheless, liquid helium often is preferred, since Fujiyoshi and colleagues have shown very clearly that it provides at least two times more protection against radiation damage than does liquid nitrogen (Fujiyoshi, 1998). Their data on cryo-protection of thin catalase crystals are reproduced in Fig. 3, and show quantitatively the importance of evaluating multiple different temperature levels, in order to determine the exact degree of protection provided by the two cryogens (Fujiyoshi, 1998). Since a better level of cryo-protection is detected with liquid helium at 4–8 K *versus* 20 K (Fig. 3), these results strongly emphasize the need to attribute measured cryo-protection with liquid helium to specific temperatures rather than to the entire temperature range available with this cryogen; they also indicate that failure to obtain positive findings for better protection over liquid nitrogen at some liquid-helium temperatures (*e.g.* 50 K) is inconclusive, since tests at 4 K or lower are required to validate any true negative conclusion. The practical importance of improved specimen preparation and the anti-damage capability of liquid helium is illustrated by the recent notable advance in resolution of membrane protein structure to 1.9 Å (Gonen *et al.*, 2005), finally surpassing the 3 Å value that has stood unbroken for many years.

The protection against radiation damage offered by liquid cryogens is often used in TEM/TED to permit data recording with a higher SNR than would be tolerated otherwise. A longer exposure (*i.e.* a higher dose) can be utilized with cryo-protection by liquid helium than with cooling by liquid nitrogen; similarly, a higher dose can be utilized with liquid helium protection at 4 K or less, than at 20–50 K.

### 5.4. New technical developments might provide additional reduction in electron radiation damage

It often is frustrating to recognize that the resolution levels now achieved for most protein specimens with studies in electron cryo-microscopes are worse than those rather routinely produced by X-ray diffraction. To obtain the highly ordered 3-D crystals needed for X-ray diffraction, a simple or complex mixture of buffer, salts, and special additives typically is used to promote crystallization; yet other compounds are often added before the crystals are cryo-cooled (*e.g.* conformational trappers, cosmotropes, cryo-protectant agents, protein stabilizers, *etc.*) (*e.g.* Heras & Martin, 2005). This 'mother liquor' (see reviews by Sousa, 1997; Giegé & McPherson, 2001) or the cryo-buffer (normally constituted of the mother liquor mixed with a cryoprotectant agent such as glycerol) usually is partially retained around the crystal during its cooling and actual X-ray beam exposure. Thus, a very supportive and protective environment (in addition to the use of low-temperature-based protection and limited radiation doses) is provided for protein crystals being subjected to X-ray diffraction. This is in great contrast to the frozen-hydrated samples prepared for electron cryo-microscopy, since the latter are usually surrounded only by vitreous ice or vitrified buffer; similarly, most supported specimens are dried within only a simple sugar solution. Development of a protective matrix analogous to mother liquors and cryo-buffers should benefit sample stability and radiation resistance during TED and TEM, and could thereby facilitate obtaining protein structure at somewhat better resolution levels than are achieved at present. An important feature of this concept will be to include anti-damage additives (*e.g.* anti-oxidants, free-radical scavengers, stabilizers) which can quench free-radicals and thereby decrease the amount of secondary radiation damage beyond that produced by the well developed means described above. Some structure-preserving saccharides also have anti-oxidative properties (*e.g.* Benaroudj *et al.*, 2001), meaning that dual functional capabilities can be given by certain individual additives.

Damage from electron beam irradiation is most frequently detected either by measuring the progressive decrease in intensity of Bragg reflections from a thin crystal as a function of accumulated dose (*e.g.* Hayward & Glaeser, 1979), or determining the resolution level for a 2-D or 3-D reconstruction of polypeptide structure (*e.g.* Conway *et al.*, 1993). Recently, a much simpler and faster means for direct detection of this damage has been recognized: imaging of radiation-induced bubble formation within a thin amorphous layer of dry sodium phosphate buffer (Massover, 2006*a*); an example is shown in Fig. 4. The small spherical bubbles arising from electron irradiation typically go through a sequence of nucleation, growth, possible fusion, and stable end-state. The identity of the gas inside these bubbles is as yet unknown. Beam-induced bubbles of hydrogen gas formed within vitreous ice have been reported previously (Leapman & Sun, 1995); a recent study has noted that this bubbling response in vitreous ice differs at 12 K from that at 82 K (Wright *et al.*, 2006). Sodium ascorbate, a well-known anti-oxidant, when mixed with sodium phosphate buffer, decreases and modifies the bubbling response to electron irradiation (Massover, 2006*b*). The facile direct detection of electron radiation damage in dry sodium phosphate buffer should be useful as a model system to identify effective anti-damage additives and new protocols that could protect polypeptides from radiation damage to a better extent.

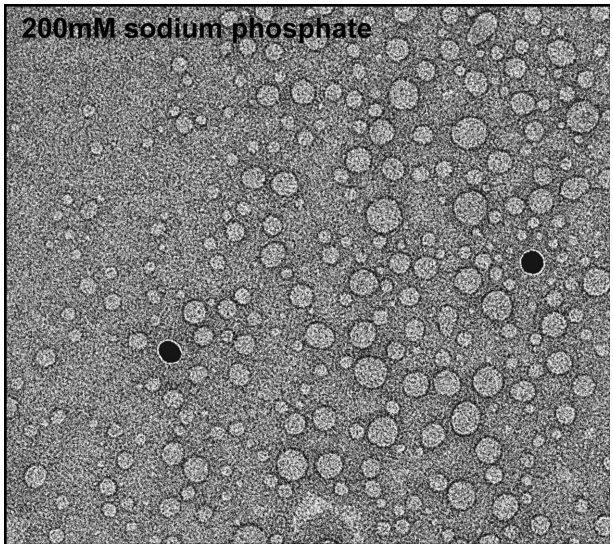


**Figure 4**
Electron-beam-induced bubbling in dry sodium phosphate. The amorphous salt layer is thinner to the upper left, and thicker to the lower right. The number and size range of spherical bubbles increases with thickness of the dry salt; adjacent areas that are even thinner show no bubbles. The image is intentionally underfocused to increase phase contrast. Dark dots are 15 nm colloidal gold particles.

## 6. Can additional measures be taken to reduce radiation damage from synchrotron X-ray sources?

Radiation damage presently compromises protein structure determination by X-ray diffraction at third-generation synchrotron facilities despite the use of cryo-cooling to protect specimens (Carugo & Carugo, 2005; Nave & Garman, 2005). Although X-ray photons and fast electrons have major physical differences, the mechanisms by which they cause radiation damage during the structure determination of protein specimens are quite similar (Henderson, 1990; Glaeser *et al.*, 2000). Hence, it is very appropriate to consider whether any of the well developed anti-damage strategies now routinely employed during electron diffraction and imaging can be usefully applied to help limit radiation damage in MX.

With regard to *instrumentation*, the tuning of X-ray wavelength (*i.e.* as used for maximizing anomalous signal intensities during acquisition of MAD or SAD data for phasing) is formally analogous to the use of smaller and faster electrons produced by higher accelerating voltages in electron microscopes. Longer X-ray wavelengths are known to increase absorption. The actual extent of the potential advantage of tuning the X-ray wavelength for the specific purpose of trying to reduce radiation damage still is being debated and evaluated experimentally [*e.g.* Nave & Hill, 2005; Weiss *et al.*, 2005; Shimizu *et al.*, 2007 (in this issue)]. Further experimental tests studying use of different wavelengths are needed and probably should be subdivided to examine global radiation damage, or defined structural changes to specific amino acids.

With regard to using *low-dose exposures* to record diffraction data, there is much current activity at synchrotron facilities to investigate exactly which dose levels and regimens can be tolerated before protein structure is compromised by radiation damage (*e.g.* Sliz *et al.*, 2003; Boutet & Robinson, 2006; Owen *et al.*, 2006). Although it now is widely recognized that some X-ray diffraction structures entered into the protein database are describing damaged polypeptides, there still seems to be very little experimental utilization at synchrotron facilities of all four requirements of the low-dose concept developed for electron beam studies (see §5.2). In particular, synchrotron diffraction data are infrequently collected at truly minimal SNR; hence, the potential value of this practice is unclear. Development of efficient means to record series of fractionated doses with sufficiently restricted intensity at synchrotron beamlines will facilitate this determination; since third-generation synchrotron sources have very high intensities, such experiments will probably require the use of very short time intervals for each exposure and/or the use of beam attenuation. Only when specific experimental data become available will it be possible to develop more general recommendations for possible research usage of full low-dose recording at synchrotron facilities.

Currently, almost all crystallography at synchrotron centers uses *specimen protection* by cooling with a nitrogen gas cryostream (see reviews by Hope, 1988, 2001; Garman & Owen, 2006). This means that there are several major practical differences with cryo-cooling for MX at synchrotron facilities compared with the cryo-protection now practiced for electron beam imaging and diffraction. At synchrotron beamlines, (i) specimens are not kept inside a high vacuum, (ii) specimen temperature is not maintained by metallic conduction directly linked to the liquid cryogen, and (iii) liquid helium is not used as the cryogen. Clearly, changing everything to match the conditions routinely used for cryo-protection in TED/TEM would require large engineering efforts and expenses; hence, practical interest is initially centered around the question of which cryogen gives better protection.

Use of liquid helium with electron beam studies provides at least two times better specimen protection than is obtained with liquid nitrogen (Fujiyoshi, 1998). Although the potential value of using liquid helium rather than liquid nitrogen for cryo-protection at high-intensity X-ray sources is being discussed actively, there have been only limited experimental investigations published to date (*e.g.* Hanson *et al.*, 2002; Teng & Moffat, 2002). Very sensitive spectroscopic assays of photosystem II have shown that synchrotron radiation damage to the manganese complex can be decreased by as much as 50% at 10 K compared with that produced at 100 K (Yano *et al.*, 2005; Grabolle *et al.*, 2006). Since the hoped-for benefits of liquid helium with MX have not yet become convincing, one must remain cognizant that the low temperatures being examined usually did not extend down to 4 K or even less, and thus these evaluations must be considered to be incomplete. Before adoption of liquid helium cryo-cooling and cryo-protection at synchrotron facilities could be recommended for general use, experimental proof must be obtained that a sufficient benefit in reducing structural damage is produced; only such a practical demonstration will be convincing enough to justify the engineering and expense of installing efficient superfluid liquid-helium systems.

In this regard, it should be recognized that the liquid helium systems now used for cryo-TEM/TED are based on an extensive history of worldwide developmental efforts. The modern 'very easy' cryostats required much new engineering and many iterative changes over a period of many years (see review by Fujiyoshi, 1998). An important part of the successful cryostat design worked out by Fujiyoshi and colleagues (Fujiyoshi *et al.*, 1991) is the use of a closed-cycle system for helium recirculation; this feature substantially lessens the expenses for daily operation, and differs to an enormous extent from the open gas systems presently used for specimen cooling at synchrotron facilities. It seems likely that a full experimental evaluation of liquid helium for sample cryoprotection in MX would be facilitated by having the protein crystal specimens kept inside a vacuum chamber, rather than being within an open jet of cold gas flowing into the atmosphere; thus, the three differences listed above unfortunately are seen to be intertwined to a large extent.

With regard to *specimen environment*, the idea of adding chemical compounds that can interact with damage mechanisms to block or decrease radiation-induced changes in protein structure goes back to an early X-ray diffraction study by Sarma & Zaloga (1975) using a styrene additive. Several different anti-oxidants and free-radical scavengers now have been shown to give protection and increased life-times for protein crystals during synchrotron irradiation [Murray & Garman, 2002; Kauffmann *et al.*, 2006; Southworth-Davies & Garman, 2007 (in this issue)]. Sufficient time for the experimental evaluation of other compounds will be needed to identify the best anti-damage additives, and to test whether a multi-component cocktail suitable for routine usage in MX can be formulated; use of a cocktail approach is supported by the report that a mixture of the structure-supporting sugar, glucose, with a derivatized saccharide, tannate, gives notably better results for electron cryo-diffraction of tubulin monolayer crystals than did specimens prepared with either component by itself (Nogales *et al.*, 1995).

Synchrotron crystallographers should recognize from this discussion that several additional means to reduce the effects of X-ray radiation damage upon protein structure are indeed available. Although it might seem unlikely that any single change will dramatically improve protection of protein samples subjected to third-generation synchrotron irradiation, incremental smaller improvements resulting from several different changes in current practices could add up to significantly lessen the amount of X-ray radiation damage. All of the ideas for potential benefits discussed here clearly require convincing experimental testing and validation; final judgments about theoretical benefits always must be based upon tests under real-life conditions. In addition, any new evidence for improved protection of protein specimens must then be translated either to show significantly reduced radiation damage occurring with common dose regimens (*i.e.* longer crystal life-time), or to allow use of higher doses without increasing the radiation damage. Hopefully, experimentalists will be stimulated to undertake the necessary evaluations.

## 7. Conclusions and perspectives

I conclude that there are several possibilities to further reduce the destructive actions of radiation damage in synchrotron crystallography. All these require experimental testing to evaluate which can actually provide concrete benefits for polypeptide structure determination. The consequent developmental costs and engineering efforts are justified by the large importance of solving this practical problem.

Can any new directions going even beyond those described above be encouraged? I believe that the answer is yes, with regard to both X-rays and electrons.

(i) Develop a cocktail of anti-damage additives that will *stop or reduce specific, rather than general, damage* caused by the irradiation. The increased knowledge about preferential changes to certain amino acids commonly produced by synchrotron X-ray beams (*e.g.* decarboxylation of aspartate and glutamate, dehydroxylation of tyrosine, reduction of disulfide bonds, *etc.*) (Burmeister, 2000; Ravelli & McSweeney, 2000; Weik *et al.*, 2000; Carugo & Carugo, 2005; Nave & Garman, 2005) provides a very good basis for testing this idea.

(ii) *Develop means to dry 3-D protein crystals* (*e.g.* freeze-dried, or supported by a sugar matrix). The absence of water/ice in such dry crystals will prevent several radiolytic mechanisms that normally generate free-radicals, and will thus decrease secondary radiation damage (*e.g.* Nave & Hill, 2005). Simultaneously, this gas- and ice-free state will usefully decrease the X-ray background for anomalous signals having low intensity (*e.g.* Glaeser *et al.*, 2000). Dehydration is a well known method that can increase crystal quality (see review by Heras & Martin, 2005). However, whether 3-D protein crystals can tolerate actual drying while leaving native polypeptides intact within the full volume of the highly ordered lattice is not yet clear, although preliminary experiments on this have recently been carried out and show promise [Ravelli *et al.*, 2007 (in this issue)].

(iii) *Design new software* that can take a high-resolution 3-D reconstruction and convert the observed damaged structure back to its pre-irradiated native state. Although this proposal might seem wildly speculative and even unrealistic, some software already has been developed that corrects MX data back towards the initial structure factors (*e.g.* Diederichs, 2006; Diederichs *et al.*, 2003; Schiltz *et al.*, 2004). To be fully developed, this idea necessarily depends upon first obtaining a total knowledge about all the specific structural changes caused by the irradiation, and about the probabilities for each change at a given dose. The final result of using such software would be generation of a theoretical undamaged counterpart to a newly determined, but damaged, structure. This computational approach will be of particular value for both electron and X-ray beams if it turns out that certain radiation-induced specific changes in polypeptide structure cannot be avoided despite the use of advanced countermeasures.

The successful development and testing of these or yet other unconventional possibilities to deal more effectively with radiation damage from synchrotron beams (*e.g.* Nave & Hill, 2005) will be greatly facilitated by much more vigorous

interactive communications between X-ray diffractionists and members of all the other research groups involved with this very important practical problem (*i.e.* electron crystallographers, instrumentation engineers, radiation chemists, radiation physicists, software programmers, *etc.*). The ongoing Radiation Damage Workshops are a good foundation to facilitate the needed discussions and debates.

This material was presented orally at the session on 'Experiences from Electron Microscopy' during the Fourth International Workshop on the X-ray Damage to Biological Crystalline Samples (SPring-8, Harima, Japan) in March 2006. I thank Dr Thomas Walz and coauthors (Department of Cell Biology, Harvard Medical School, Boston, MA 02115, USA) for permission to reproduce Fig. 1. I thank Dr Steven J. Ludtke and coauthors (National Center for Macromolecular Imaging, Department of Biochemistry and Molecular Biology, Baylor College of Medicine, Houston, TX 77030, USA) for permission to reproduce Fig. 2. I thank Professor Yoshinori Fujiyoshi (Department of Biophysics, Kyoto University, Kyoto 606-8502, Japan) for permission to reproduce Fig. 3. Lastly, I also thank many colleagues working with either electrons or X-rays for helpful discussions.

## References


Adams, B., Nishino, Y. & Materlik, G. (2000). *J. Synchrotron Rad.* **7**, 274–279.

Adrian, M., Dubochet, J., Lepault, J. & McDowell, A. W. (1984). *Nature (London)*, **308**, 32–36.

Allison, S. D., Chang, B., Randolph, T. W. & Carpenter, J. F. (1999). *Arch. Biochem. Biophys.* **365**, 289–298.

Baumeister, W. & Steven, A. C. (2000). *Trends Biochem. Sci.* **25**, 624–631.

Belnap, D. M., Kumar, A., Folk, J. T., Smith, T. J. & Baker, T. S. (1999). *J. Struct. Biol.* **125**, 166–175.

Benaroudj, N., Lee, D. H. & Goldberg, A. L. (2001). *J. Biol. Chem.* **276**, 24261–24267.

Boutet, S. & Robinson, I. K. (2006). *J. Synchrotron Rad.* **13**, 1–7.

Braig, K., Adams, P. D. & Brunger, A. T. (1995). *Nature Struct. Biol.* **2**, 1083–1094.

Bullough, P. & Henderson, R. (1987). *Ultramicroscopy*, **21**, 223–230.

Burmeister, W. P. (2000). *Acta Cryst.* D**56**, 328–341.

Carugo, O. & Carugo, K. D. (2005) *Trends Biochem. Sci.* **30**, 213–219.

Chapman, H. N., Barty, A., Marchesini, S., Noy, A., Hau-Riege, S. P., Cui, C., Howells, M. R., Rosen, R., He, H., Spence, J. C., Weierstall, U., Beetz, T., Jacobsen, C. & Shapiro, D. (2006). *J. Optic. Soc. Am. A*, **23**, 1179–1200.

Chiu, W. (2001). *International Tables of Crystallography*, Vol. F, edited by M. G. Rossman and E. Arnold, pp. 423–427. Dordrecht: Kluwer.

Chiu, W., Baker, M. L. & Almo, S. C. (2006). *Trends Cell Biol.* **16**, 144–150.

Chiu, W., Baker, M. L., Jiang, N., Dougherty, M. & Schmidt, M. F. (2005). *Structure*, **13**, 363–372.

Chiu, W. & Rixon, F. J. (2002). *Virus Res.* **82**, 9–17.

Comolli, L. R. & Downing, K. H. (2005). *J. Struct. Biol.* **152**, 149–156.

Conway, J. F., Trus, B. L., Booy, F. P., Newcomb, W. N., Brown, J. C. & Steven, A. C. (1993). *J. Struct. Biol.* **111**, 222–233.

Cosslett, V. E. (1978). *J. Microsc. Oxford*, **113**, 113–129.

Crowe, L. M. (2002). *Comput. Biochem. Physiol. Part A*, **131**, 303–319.

DeRosier, D. J. & Moore, P. B. (1970). *J. Mol. Biol.* **52**, 355–369.

Diederichs, K. (2006). *Acta Cryst.* D**62**, 96–101.

Diederichs, K., McSweeney, S. & Ravelli, R. B. G. (2003). *Acta Cryst.* D**59**, 903–909.

Downing, K. H. (1991). *Science*, **251**, 53–59.

Downing, K. H. & Glaeser, R. M. (1986). *Ultramicroscopy*, **20**, 269–278.

Dubochet, J., Adrian, M., Chang, J. J., Homo, J. C., Lepault, J., McDowall, A. W. & Schultz, P. (1988). *Q. Rev. Biophys.* **21**, 129–228.

Egerton, R. F., Li, P. & Malac, M. (2004). *Micron*, **35**, 399–409.

Eisebitt, S., Lüning, J., Schlotter, W. F., Lörgen, M., Hellwig, O., Eberhardt, W. & Stöhr, J. (2004). *Nature (London)*, **432**, 885–888.

Ennifar, E., Carpentier, P., Ferrer, J.-L., Walter, P. & Dumas, P. (2002). *Acta Cryst.* D**58**, 1262–1268.

Fabiola, F. & Chapman, M. S. (2005). *Structure*, **13**, 389–400.

Faruqi, A. R. & Subramaniam, S. (2000). *Q. Rev. Biophys.* **33**, 1–27.

Fleishman, S. J., Unger, V. M. & Ben-Tal, N. (2006). *Trends Biochem. Sci.* **31**, 106–112.

Frank, J. (2002). *Ann. Rev. Biophys. Biomol. Struct.* **31**, 303–319.

Fujiyoshi, Y. (1998). *Adv. Biophys.* **35**, 25–80.

Fujiyoshi, Y. (2006). *Proceedings of the 16th International Microscopy Congress*, Vol. 1, p. 207, 3–8 September 2006, Sapporo, Japan.

Fujiyoshi, Y. Mizusaki, T., Morikawa, K., Yamagishi, H., Aoki, Y., Kihara, H. & Harada, Y. (1991). *Ultramicroscopy*, **38**, 241–251.

Garman, E. F. & Owen, R. L. (2006). *Acta Cryst.* D**62**, 32–47.

Giegé, R. & McPherson, A. (2001). *International Tables of Crystallography*, Vol. F, edited by M. G. Rossman and E. Arnold, pp. 81–93. Dordrecht: Kluwer.

Glaeser, R., Facciotti, M., Walian, P., Rouhani, S., Holton, J., MacDowell, A., Celestre, R., Cambie, D. & Padmore, H. (2000). *Biophys. J.* **78**, 3178–3185.

Glaeser, R. M. (1999). *J. Struct. Biol.* **128**, 3–14.

Glykos, N. M., Holzenburg, A. & Phillips, S. E. V. (1998). *Acta Cryst.* D**54**, 215–225.

Gonen, T., Cheng, Y., Sliz, P., Hiroaki, Y., Fujiyoshi, Y., Harrison, S. C. & Walz, T. (2005). *Nature (London)*, **438**, 633–638.

Grabolle, M., Haumann, M., Müller, C., Liebisch, P. & Dau, H. (2006). *J. Biol. Chem.* **281**, 4580–4588.

Grimes, J. M., Fuller, S. D. & Stuart, D. I. (1999). *Acta Cryst.* D**55**, 1742–1749.

Gyobu, N., Tani, K., Hiroaki, Y., Kamegawa, A., Mitsuoka, K. & Fujiyoshi, Y. (2004). *J. Struct. Biol.* **146**, 325–333.

Hanson, B. L., Harp, J. M., Kirschbaum, K., Schall, C. A., DeWitt, K., Howard, A., Pinkerton, A. H. & Bunick, G. J. (2002). *J. Synchrotron Rad.* **9**, 375–381.

Harms, J., Tocilj, A., Levin, I., Agmon, I., Stark, H., Kölln, I., van Heel, M., Cuff, M., Schlünzen, F., Bashan, A., Franceschi, F. & Yonath, A. (1999). *Structure*, **7**, 931–941.

Hayward, S. B. & Glaeser, R. M. (1979). *Ultramicroscopy*, **4**, 201–210.

Henderson, R. (1990). *Proc. R. Soc. London Ser. B*, **241**, 6–8.

Henderson, R. (1995). *Q. Rev. Biophys.* **28**, 171–193.

Henderson, R. (2004). *Q. Rev. Biophys.* **37**, 3–13.

Heras, B. & Martin, J. L. (2005). *Acta Cryst.* D**61**, 1173–1180.

Hirai, T., Murata, K., Mitsuoka, K., Kimura, Y. & Fujiyoshi, Y. (1999). *J. Electron Microsc.* **48**, 653–658.

Hope, H. (1988). *Acta Cryst.* B**44**, 22–26.

Hope, H. (2001). *International Tables of Crystallography*, Vol. F, edited by M. G. Rossman and E. Arnold, pp. 197–201. Dordrecht: Kluwer.

Huldt, G., Szoke, A. & Hajdu, J. (2003). *J. Struct. Biol.* **144**, 219–227.

Iancu, C. V., Wright, E. R., Heymann, J. B. & Jensen, G. J. (2006). *J. Struct. Biol.* **153**, 231–240.

International Study Group (1986). *J. Microsc. Oxford*, **141**, 385–391.

Jap, B., Zylauf, M., Scheybani, T., Hefti, A., Baumeister, W., Aebi, U. & Engel, A. (1992). *Ultramicroscopy*, **46**, 45–84.

Kauffmann, B., Weiss, M. S., Lamzin, V. S. & Schmidt, A. (2006). *Structure*, **14**, 1099–1105.

Kaushik, J. K. & Bhat, R. (2003). *J. Biol. Chem.* **278**, 26458–26465.
Kimura, Y., Vassylyev, D. G., Miyazawa, A., Kidera, A., Matsushima, M., Mitsuoka, K., Murata, K., Hirai, T. & Fujiyoshi, Y. (1997). *Nature (London)*, **389**, 206–211.
Kühlbrandt, W. (1992). *Q. Rev. Biophys.* **25**, 1–49.
Kühlbrandt, W. & Williams, K. A. (1999). *Curr. Opin. Chem. Biol.* **3**, 537–543.
Kuwamoto, S., Akiyama, S. & Fujisawa, T. (2004). *J. Synchrotron Rad.* **11**, 462–468.
Leapman, R. D. & Sun, S. (1995). *Ultramicroscopy*, **59**, 71–79.
Lei, J. L. & Frank, J. (2005). *J. Struct. Biol.* **150**, 69–80.
Liljas, A. (2006). *Acta Cryst.* D**62**, 941–945.
Lippert, K. & Galinski, E. A. (1992). *Appl. Microbiol. Biotechnol.* **37**, 61–65.
Löwe, J., Li, H., Downing, K. H. & Nogales, E. (2001). *J. Mol. Biol.* **313**, 1045–1051.
Ludtke, S. J., Chen, D-H., Song, J-L., Chuang, D. J. & Chiu, W. (2004). *Structure*, **12**, 1129–1136.
Massover, W. H. (2006*a*). *Microsc. Microanal.* **12** (Suppl. 2), 390CD–391CD.
Massover, W. H. (2006*b*). *Proceedings of the 16th International Microscopy Congress*, Vol. 1, p. 492, 3–8 September 2006, Sapporo, Japan.
Miao, J., Hodgson, K. O. & Sayre, D. (2001). *Proc. Natl. Acad. Sci. USA*, **98**, 6641–6645.
Miao, J., Kirz, J. & Sayre, D. (2000). *Acta Cryst.* D**56**, 1312–1315.
Mitra, K. & Frank, J. (2006). *Ann. Rev. Biophy. Biomol. Struct.* **35**, 299–317.
Murray, J. & Garman, E. (2002). *J. Synchrotron Rad.* **9**, 347–359.
Nave, C. & Garman, E. F. (2005). *J. Synchrotron Rad.* **12**, 257–260.
Nave, C. & Hill, M. A. (2005). *J. Synchrotron Rad.* **12**, 299–303.
Nogales, E., Wolf, S. G., Zhang, S. X. & Downing, K. (1995). *J. Struct. Biol.* **115**, 199–208.
Novikov, D. V., Adams, B., Hiort, T., Kossel, E., Materlik, G., Menk, R. & Walenta, A. (1998). *J. Synchrotron Rad.* **5**, 315–319.
Orlova, E. V. (2000). *Acta Cryst.* D**56**, 1253–1258.
Owen, C. H., Morgan, D. G. & DeRosier, D. J. (1996). *J. Struct. Biol.* **116**, 167–175.
Owen, R. L., Rudiño-Piñera, R. & Garman, E. F. (2006). *Proc. Natl. Acad. Sci. USA*, **103**, 4912–4917.
Prestrelski, S. J., Tedeschi, N., Arakawa, T., & Carpenter, J. F. (1993). *Biophys. J.* **65**, 661–671.
Ravelli, R. B. G., Haselmann-Weiss, U., McGeehan, J. E., McCarthy, A. A., Marquez, J. A., Antony, C., Frangakis, A. S. & Stranzl, G. (2007). *J. Synchrotron Rad.* **14**, 128–132.
Ravelli, R. B. G. & McSweeney, S. M. (2000). *Structure*, **8**, 315–328.
Ren, G., Cheng, H., Reddy, V., Melnyk, P. & Mitra, A. K. (2000). *J. Mol. Biol.* **301**, 369–387.
Rose, A. (1948). *Adv. Electronics Electron Phys.* **1**, 131–166.
Rossman, M. G., Bernal, R. & Ploetnev, S. V. (2001). *J. Struct. Biol.* **136**, 190–200.
Rossman, M. G., Morais, M. C., Leiman, P. G. & Zhang, W. (2005). *Structure*, **13**, 355–362.
Ruprecht, J. & Nield, J. (2001). *Prog. Biophys. Mol. Biol.* **75**, 121–164.
Saibil, H. R. (2000). *Acta Cryst.* D**56**, 1215–1222.
Sarma, R. & Zaloga, G. (1975). *J. Mol. Biol.* **98**, 479–484.
Schiltz, M., Dumas, P., Ennifar, E., Flensburg, C., Paciorek, W., Vonrhein, C. & Bricogne, G. (2004). *Acta Cryst.* D**60**, 1024–1031.
Shimizu, N., Hirata, K., Hasegawa, K., Ueno, G. & Yamamoto, M. (2007). *J. Synchrotron Rad.* **14**, 4–10.
Sliz, P., Harrison, S. C. & Rosenbaum, G. (2003). *Structure*, **11**, 13–19.
Sousa, R. (1997). *Methods Enzymol.* **276**, 131–143.
Southworth-Davies, R. L. & Garman, E. F. (2007). *J. Synchrotron Rad.* **14**, 73–83.
Stagg, S. M., Lander, G. C., Pulokas, J., Fellmann, D., Cheng, A. C., Quispe, J. D., Mallick, S. P., Avila, R. M., Carragher, B. & Potter, C. S. (2006). *J. Struct. Biol.* **155**, 470–481.
Steinmetz, M. O., Hoenger, A., Tittman, P., Fuchs, K. H., Gross, H. & Aebi, U. (1998). *J. Mol. Biol.* **278**, 703–711.
Steven, A. C., Trus, B. L., Booy, F. P., Cheng, N., Zlotnick, A., Caston, J. R. & Conway, J. F. (1997). *FASEB J.* **11**, 733–742.
Subramaniam, S. & Milne, J. L. S. (2004). *Ann. Rev. Biophys. Biomol. Struct.* **33**, 141–155.
Suloway, C., Pulokas, J., Fellmann, D., Cheng, A., Guerra, F., Quispe, J., Stagg, S., Potter, C. S. & Carragher, B. (2005). *J. Struct. Biol.* **151**, 41–60.
Tang, L. & Johnson, J. E. (2002). *Biochemistry* **41**, 11517–11524.
Teng, T-Y. & Moffat, K. (2002). *J. Synchrotron Rad.* **9**, 198–201.
Unwin, N. (2005). *J. Mol. Biol.* **346**, 967–989.
Unwin, P. N. T. & Henderson, R. (1975). *J. Mol. Biol.* **94**, 425–440.
Uritani, M., Takai, M. & Yoshinaga, K. (1995). *J. Biochem.* **117**, 774–779.
Van Heel, M., Gowen, B., McYacheen, R., Orlova, E. V., Finn, R., Pape, T., Cohen, D., Stark, H., Schmidt, R., Schatz, M. & Patwardhan, A. (2000). *Q. Rev. Biophys.* **33**, 307–369.
Wang, D. N. & Kühlbrandt, W. (1991). *J. Mol. Biol.* **217**, 691–699.
Weik, M., Ravelli, R. B. G., Kryger, G., McSweeney, S., Raves, M. L., Harel, M., Goos, P., Silman, I., Kroon, J. & Sussman, J. L. (2000). *Proc. Natl. Acad. Sci. USA*, **97**, 623–628.
Weiss, M. S., Panjikar, S., Mueller-Dieckmann, C. & Tucker, P. A. (2005). *J. Synchrotron Rad.* **12**, 304–309.
Wriggers, W., Milligan, R. A. & McCammon, J. A. (1999). *J. Struct. Biol.* **125**, 185–195.
Wright, E. R., Iancu, C. V., Tivol, W. F. & Jensen, G. J. (2006). *J. Struct. Biol.* **153**, 241–252.
Wu, X., Milne, J. L. S., Borgnia, M. J., Rostapshov, A. V., Subramaniam, S. & Brooks, B. R. (2003). *J. Struct. Biol.* **141**, 63–76.
Yaeger, M., Unger, V. M. & Mitra, A. K. (1999). *Methods Enzymol.* **294**, 135–180.
Yano, J., Kern, J., Irrgang, K-D., Latimer, M. J., Bergmann, U., Glatzel, P., Pushkar, Y., Biesiadka, J., Loll, B., Sauer, K., Messinger, J., Zouni, A. & Yachandra, V. K. (2005). *Proc. Natl. Acad. Sci. USA*, **102**, 12047–12052.
Yonekura, K., Maki-Yonekura, S. & Namba, K. (2005). *Structure*, **13**, 407–412.